J|A|C|S ARTICLES

Published on Web 08/12/2010

Luminescent Au(I)/Cu(I) Alkynyl Clusters with an Ethynyl Steroid and Related Aliphatic Ligands: An Octanuclear Au_4Cu_4 Cluster and Luminescence Polymorphism in Au_3Cu_2 Clusters

Gerald F. Manbeck,[†] William W. Brennessel,[†] Robert A. Stockland, Jr.,[‡] and Richard Eisenberg*,[†]

Department of Chemistry, University of Rochester, Rochester, New York 14627, and Department of Chemistry, Bucknell University, Lewisburg, Pennsylvania 17837

Received April 21, 2010; E-mail: eisenberg@chem.rochester.edu

Abstract: Gold(I) bis(acetylide) complexes [PPN][AuR_2] (**1**−**3**) where PPN = bis(triphenylphosphine)iminium) and R = ethisterone (**1**); 1-ethynylcyclopentanol (**2**); 1-ethynylcyclohexanol (**3**) have been prepared. The reaction of **1** with [$Cu(MeCN)_4$][PF_6] in a 1:1 or 3:2 ratio provides the octanuclear complex [Au_4Cu_4-(ethisterone)$_8$] (**4**) or pentanuclear complex [PPN][Au_3Cu_2(ethisterone)$_6$] (**5**). Complexes **2** and **3** react with [$Cu(MeCN)_4$][PF_6] to form only pentanuclear Au(I)/Cu(I) complexes [PPN][Au_3Cu_2(1-ethynylcyclopentanol)$_6$] (**6**) and [PPN][Au_3Cu_2(1-ethynylcyclohexanol)$_6$] (**7**). X-ray crystallographic studies of **1**−**3** reveal nontraditional hydrogen bonding between hydroxyl groups and the acetylide units of adjacent molecules. Complexes **6** and **7** each form polymorphs in which the structures (**6 a**,**b** and **7 a,b,c**) differ by Au···Au, Au···Cu, and Cu−C distances. The polymorphs exhibit different emission energies with colors ranging from blue to yellow in the solid state. In solution, pentanuclear clusters **5**−**7** emit with λ_{max} = 570−580 nm and Φ = 0.05−0.19. Complex **4** emits at 496 nm in CH_2Cl_2 with a quantum yield of 0.65. Complex **5** exists in equilibrium with **1** and **4** in the presence of methanol, ethanol, ethyl acetate, or water. This equilibrium has been probed by X-ray crystallography, NMR spectroscopy, and luminescence experiments. DFT calculations have been performed to analyze the orbitals involved in the electronic transitions of **4**, **6**, and **7**.

Introduction

Among polynuclear d^{10} complexes,[1−6] examples incorporating Au(I) acetylide units bound to Cu(I) or Ag(I) ions in an η^2 fashion have emerged as an interesting set of systems that often exhibit intense photoluminescence.[7−15] In these compounds, emission may be modified not only by aurophilic Au···Au interactions[16−18] but also by the potential for Au···Cu or Au···Ag interactions between these closed-shell d^{10} ions. One strategy for the preparation of such compounds is the simple addition of Cu(I) or Ag(I) ions to dinuclear phosphine-bridged Au(I) acetylide complexes. In this context, Yam and co-workers have shown that (1,1′-bis(diphenylphosphino)ferrocene)Au(I) acetylides react with [$Cu(MeCN)_4$]PF_6 or AgOTf in a 1:1 ratio to form what was postulated as a trinuclear Au_2M (M = Ag or Cu) complex (**I**).[15] Weakened C≡C stretching frequencies and red-shifted emission relative to the Au(I) precursors were consistent with η^2-coordination of the acetylide ligand to Ag(I) or Cu(I). Structural characterization was absent for these complexes, and therefore, the exact arrangement of Au(I) and Cu(I) ions was not known.

[†] University of Rochester.
[‡] Bucknell University.

(1) Yam, V. W. W.; Lo, K. K. W. *Chem. Soc. Rev.* **1999**, *28*, 323.
(2) Yam, V. W. W.; Lo, K. K. W.; Fung, W. K. M.; Wang, C. R. *Coord. Chem. Rev.* **1998**, *171*, 17.
(3) Wang, Q. M.; Lee, Y. A.; Crespo, O.; Deaton, J.; Tang, C.; Gysling, H. J.; Gimeno, M. C.; Larraz, C.; Villacampa, M. D.; Laguna, A.; Eisenberg, R. *J. Am. Chem. Soc.* **2004**, *126*, 9488.
(4) Barbieri, A.; Accorsi, G.; Armaroli, N. *Chem. Commun.* **2008**, 2185.
(5) Packheiser, R.; Jakob, A.; Ecorchard, P.; Walfort, B.; Lang, H. *Organometallics* **2008**, *27*, 1214.
(6) Yam, V. W. W.; Cheung, K. L.; Yip, S. K.; Cheung, K. K. *J. Organomet. Chem.* **2003**, *681*, 196.
(7) Koshevoy, I. O.; Smirnova, E. S.; Domenech, A.; Karttunen, A. J.; Haukka, M.; Tunik, S. P.; Pakkanen, T. A. *Dalton Transactions* **2009**, 8392.
(8) Koshevoy, I. O.; Lin, Y. C.; Karttunen, A. J.; Haukka, M.; Chou, P. T.; Tunik, S. P.; Pakkanen, T. A. *Chem. Commun.* **2009**, 2860.
(9) Koshevoy, I. O.; Lin, Y. C.; Karttunen, A. J.; Chou, P. T.; Vainiotalo, P.; Tunilk, S. P.; Haukka, M.; Pakkanen, T. A. *Inorg. Chem.* **2009**, *48*, 2094.
(10) Koshevoy, I. O.; Karttunen, A. J.; Tunik, S. P.; Haukka, M.; Selivanov, S. I.; Melnikov, A. S.; Serdobintsev, P. Y.; Pakkanen, T. A. *Organometallics* **2009**, *28*, 1369.
(11) Koshevoy, I. O.; Koskinen, L.; Haukka, M.; Tunik, S. P.; Serdobintsev, P. Y.; Melnikov, A. S.; Pakkanen, T. A. *Angew. Chem., Int. Ed.* **2008**, *47*, 3942.
(12) Koshevoy, I. O.; Karttunen, A. J.; Tunik, S. P.; Haukka, M.; Selivanov, S. I.; MeInikov, A. S.; Serdobintsev, P. Y.; Khodorkovskiy, M. A.; Pakkanen, T. A. *Inorg. Chem.* **2008**, *47*, 9478.
(13) de la Riva, H.; Nieuwhuyzen, M.; Fierro, C. M.; Raithby, P. R.; Male, L.; Lagunas, M. C. *Inorg. Chem.* **2006**, *45*, 1418.
(14) Lin, Y. C.; Chou, P. T.; Koshevoy, I. O.; Pakkanen, T. A. *J. Phys. Chem. A* **2009**, *113*, 9270.
(15) Yam, V. W. W.; Cheung, K. L.; Cheng, E. C. C.; Zhu, N. Y.; Cheung, K. K. *Dalton. Trans.* **2003**, 1830.
(16) Pyykko, P. *Chem. Rev.* **1997**, *97*, 597.
(17) Wang, S. G.; Schwarz, W. H. E. *J. Am. Chem. Soc.* **2004**, *126*, 1266.
(18) Schmidbaur, H. *Gold Bull.* **2000**, *33*, 3.

To obtain valuable structural information regarding complexes of this type, de la Riva, et al., prepared a dinuclear Au(I) phenylacetylide complex of 4,6-bis(diphenylphosphino)dibenzofuran (dbfphos).[13] The rigidity of the phosphine ligand was expected to allow for crystallographic characterization of the complexes. Addition of $Cu(MeCN)_4PF_6$ to [Au_2(phenylacetylide)$_2$-(μ-dbfphos)] provided a dimeric Au_4Cu_2 complex (**II**) with two Cu···Au close contacts but no Au···Au contacts. Solid-state emission of the complex (530 nm) was red-shifted from that of the Au(I) precursor (508 nm), consistent with the observations of Yam and co-workers.[15]

Another set of Au(I)/Cu(I) complexes that exhibit Au···Cu contacts less than the sum of van der Waal radii is composed of pentanuclear clusters of the formula [*n*-Bu_4N][(Au(aryl-acetylide)$_2$)$_3M_2$] (M = Ag, Cu) (**III**) (see Chart 1 for structures of I, II, and III). Prepared from a mixture of [*n*-Bu_4N][Au(aryl-acetylide)$_2$], polymeric gold(I) acetylide and copper(I) or silver(I) acetylides in modest yields,[19,20] these complexes consist of three gold bis(acetylide) anions bridged by two Cu(I) ions through π-coordination to the acetylide triple bonds. Only recently have the photophysical properties of these complexes been examined by absorption and emission spectroscopy and electronic structure calculations.[21] The authors concluded that the emission results from a mixture of cluster-centered and acetylide-to-cluster charge transfer excited states. Recently, related high nuclearity mixed Au(I)/Cu(I) complexes that contain Au(phenylacetylide)$_2^-$ units and η^2-acetylide bound Cu(I) ions have been prepared by self-assembly without prior isolation of the anionic gold(I) complexes.[9,11,12]

Chart 1

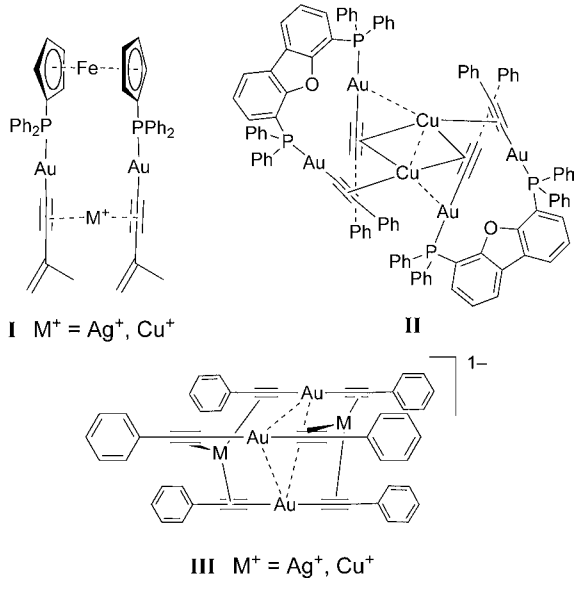

I $M^+ = Ag^+, Cu^+$ **II** **III** $M^+ = Ag^+, Cu^+$

The present study focuses on new, highly luminescent Au(I)/Cu(I) clusters in the context of potential biological interest and application. Ethisterone (17α-ethynyltestosterone) is an ethynyl steroid derivative shown below. The literature is rich in examples of organic and organometallic derivatives of estradiol[22−46] and ethisterone[47−50] that were prepared with the goal of developing therapeutic or imaging agents having significant affinity for the estrogen receptor. While the ethynyl group of ethisterone is often modified for the attachment of a transition metal, a few examples exist in which the steroid is directly coordinated to the metal as an acetylide after deprotonation[35,44,49] or through the acetylene π system.[31,48] Among them, Au(PR_3)(ethynylsteroid) complexes exemplify the same basic architecture as the gold(I) acetylide complexes mentioned above from which luminescent mixed-metal complexes are generated upon addition of Cu(I) ions. Analogues incorporating ethynylestradiol derivatives display significant binding affinities toward the estrogen receptor ligand binding domains.[49] Compounds of this type could be important considering the extensive work directed toward gold(I)

(19) Abusalah, O. M.; Alohaly, A. R. A.; Knobler, C. B. *J. Chem. Soc., Chem. Commun.* **1985**, 1502.
(20) Abusalah, O. M.; Alohaly, A. R. A. *J. Chem. Soc., Dalton Trans.* **1988**, 2297.
(21) Yip, S. K.; Chan, C. L.; Lam, W. H.; Cheung, K. K.; Yam, V. W. W. *Photochem. Photobiol. Sci.* **2007**, *6*, 365.
(22) Ferber, B.; Top, S.; Vessieres, A.; Welter, R.; Jaouen, G. *Organometallics* **2006**, *25*, 5730.
(23) Arterburn, J. B.; Corona, C.; Rao, K. V.; Carlson, K. E.; Katzenellenbogen, J. A. *J. Org. Chem.* **2003**, *68*, 7063.
(24) Top, S.; El Hafa, H.; Vessieres, A.; Huche, M.; Vaissermann, J.; Jaouen, G. *Chem.—Eur. J.* **2002**, *8*, 5241.
(25) Osella, D.; Nervi, C.; Galeotti, F.; Cavigiolio, G.; Vessieres, A.; Jaouen, G. *Helv. Chim. Acta* **2001**, *84*, 3289.
(26) Jackson, A.; Davis, J.; Pither, R. J.; Rodger, A.; Hannon, M. J. *Inorg. Chem.* **2001**, *40*, 3964.
(27) Le Bideau, F.; Kaloum, E. B.; Haquette, P.; Kernbach, U.; Marrot, J.; Stephan, E.; Top, S.; Vessieres, A.; Jaouen, G. *Chem. Commun.* **2000**, 211.
(28) Top, S.; Elhafa, H.; Vessieres, A.; Quivy, J.; Vaissermann, J.; Hughes, D. W.; McGlinchey, M. J.; Mornon, J. P.; Thoreau, E.; Jaouen, G. *J. Am. Chem. Soc.* **1995**, *117*, 8372.
(29) Vichard, D.; Gruselle, M.; Jaouen, G.; Nefedova, M. N.; Mamedyarova, I. A.; Sokolov, V. I.; Vaissermann, J. *J. Organomet. Chem.* **1994**, *484*, 1.
(30) Top, S.; Vessieres, A.; Jaouen, G. *J. Chem. Soc., Chem. Commun.* **1994**, 453.
(31) Osella, D.; Gambino, O.; Nervi, C.; Stein, E.; Jaouen, G.; Vessieres, A. *Organometallics* **1994**, *13*, 3110.
(32) Osella, D.; Dutto, G.; Jaouen, G.; Vessieres, A.; Raithby, P. R.; Debenedetto, L.; McGlinchey, M. J. *Organometallics* **1993**, *12*, 4545.
(33) Vichard, D.; Gruselle, M.; Amouri, H.; Jaouen, G.; Vaissermann, J. *Organometallics* **1992**, *11*, 2952.
(34) Vessieres, A.; Top, S.; Vaillant, C.; Osella, D.; Mornon, J. P.; Jaouen, G. *Angew. Chem., Int. Ed.* **1992**, *31*, 753.
(35) Top, S.; Gunn, M.; Jaouen, G.; Vaissermann, J.; Daran, J. C.; McGlinchey, M. J. *Organometallics* **1992**, *11*, 1201.
(36) Dizio, J. P.; Fiaschi, R.; Davison, A.; Jones, A. G.; Katzenellenbogen, J. A. *Bioconjugate Chem.* **1991**, *2*, 353.
(37) Vessieres, A.; Top, S.; Ismail, A. A.; Butler, I. S.; Louer, M.; Jaouen, G. *Biochemistry* **1988**, *27*, 6659.
(38) Savignac, M.; Jaouen, G.; Rodger, C. A.; Perrier, R. E.; Sayer, B. G.; McGlinchey, M. J. *J. Org. Chem.* **1986**, *51*, 2328.
(39) Hanson, R. N.; Friel, C. J.; Dilis, R.; Hughes, A.; DeSombre, E. R. *J. Med. Chem.* **2005**, *48*, 4300.
(40) Hanson, R. N.; Lee, C. Y.; Friel, C. J.; Dilis, R.; Hughes, A.; DeSombre, E. R. *J. Med. Chem.* **2003**, *46*, 2865.
(41) Hanson, R. N.; Lee, C. Y.; Friel, C.; Hughes, A.; DeSombre, E. R. *Steroids* **2003**, *68*, 143.
(42) Hanson, R. N.; Napolitano, E.; Fiaschi, R. *J. Med. Chem.* **1998**, *41*, 4686.
(43) Napolitano, E.; Fiaschi, R.; Herman, L. W.; Hanson, R. N. *Steroids* **1996**, *61*, 384.
(44) Sanchez-Cano, C.; Hannon, M. J. *Dalton. Trans.* **2009**, 10765.
(45) Hannon, M. J.; Green, P. S.; Fisher, D. M.; Derrick, P. J.; Beck, J. L.; Watt, S. J.; Ralph, S. F.; Sheil, M. M.; Barker, P. R.; Alcock, N. W.; Price, R. J.; Sanders, K. J.; Pither, R.; Davis, J.; Rodger, A. *Chem.—Eur. J.* **2006**, *12*, 8000.
(46) Barnes, K. R.; Kutikov, A.; Lippard, S. J. *Chem. Biol.* **2004**, *11*, 557.
(47) Top, S.; Thibaudeau, C.; Vessieres, A.; Brule, E.; Le Bideau, F.; Joerger, J. M.; Plamont, M. A.; Samreth, S.; Edgar, A.; Marrot, J.; Herson, P.; Jaouen, G. *Organometallics* **2009**, *28*, 1414.
(48) Osella, D.; Galeotti, F.; Cavigiolio, G.; Nervi, C.; Hardcastle, K. I.; Vessieres, A.; Jaouen, G. *Helv. Chim. Acta* **2002**, *85*, 2918.
(49) Stockland, R. A.; Kohler, M. C.; Guzei, I. A.; Kastner, M. E.; Bawiec, J. A.; Labaree, D. C.; Hochberg, R. B. *Organometallics* **2006**, *25*, 2475.
(50) Buil, M. L.; Esteruelas, M. A.; Garces, K.; Onate, E. *Organometallics* **2009**, *28*, 5691.

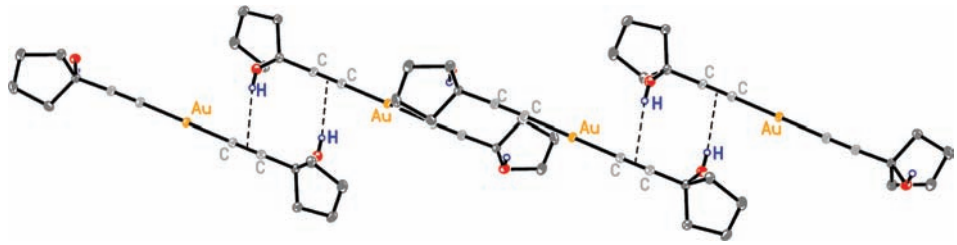

Figure 1. Packing diagram for PPN Au(1-ethynylcyclopentanol)$_2$ (**2**). PPN cations and CH_2 atoms have been omitted for clarity.

complexes as anticancer and arthritis therapy agents.[51−55] Moreover, luminescent Au(I) complexes with steroid ligands may be useful not only as hormone therapy drugs, but also for fluorescence imaging.

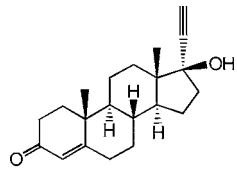

ethisterone (ethist)

In light of the relative ease of synthesizing Au(I) bis(acetylide) complexes,[56] the rich photophysical properties that have been obtained by the reaction of these Au(I) acetylide anions with Cu(I) ions, and the importance of transition metal complexes incorporating steroid units, we chose to prepare a mononuclear anionic Au(I) bis-ethisterone complex and examine its reaction with [Cu(MeCN)$_4$][PF$_6$] to form new highly luminescent complexes. In addition, we have prepared model Au(I) bis-acetylide complexes incorporating 1-ethynylcyclopentanol and 1-ethynylcyclohexanol in place of ethisterone. These simpler ethynyl alcohols were chosen for their resemblance to the steroid D-ring and the opportunity to elucidate the effect of H-bonding and steroid structure on the structural and photophysical properties of the mixed-metal Au(I)/Cu(I) ethisterone complexes. The resultant systems include an unprecedented octanuclear Au_4Cu_4 cluster and a case of luminescence polymorphism in Au_3Cu_2 clusters in which subtle differences in intramolecular Au···Au distances appear to strongly influence solid-state emission energy.

Results and Discussion

Synthesis and Crystallography. Mononuclear gold(I) bis(acetylide) salts [PPN][Au(R)$_2$] (PPN = bis(triphenylphosphine)-iminium) **1**-**3** (**1**, R = ethisterone; **2**, R = 1-ethynylcyclopentanol; **3**, R = 1-ethynylcyclohexanol) were prepared *via* the "acac method"[57] from [PPN][Au(acac)$_2$] and a slight excess of alkyne. The complexes were crystallized by vapor diffusion of ether into CH_2Cl_2 solutions and were characterized by NMR spectroscopy, microanalyses, and X-ray crystallography.

In the X-ray structures of **1**−**3**, nontraditional hydrogen bonding is observed in which hydroxylic protons are directed at the acetylide π systems of neighboring anions forming infinite chains of the Au(I) bis(acetylide) anions (Figure 1). While the geometry at gold is nearly linear in each structure, Au1−C1−C2 and Au2−C3−C4 bond angles are somewhat less than the 180° expected for sp-hybridized carbons. The effect is a curvature that is particularly noticeable in **3** where the Au1−C1−C2 and Au2−C3−C4 angles are 173.7(3)° and 167.1(4)°, respectively. The unconventional OH···π type of hydrogen bonding seen for **1**−**3** has been reported in the organometallic complex [Ni(Cp)PPh$_3$(2-methyl-3-butyn-2-ol)] in which spiral columns were formed in the extended π-bonded structure.[58]

Addition of [Cu(MeCN)$_4$](PF$_6$) to **1** in an equimolar ratio provides an octanuclear complex, [{Au(ethisterone)$_2$}$_4$Cu$_4$] (**4**), which possesses a novel Au_4Cu_4 core as described below. In contrast, when the ratio of Au:Cu in the reaction solution is changed to 3:2, a pentanuclear complex is obtained as the PPN$^+$ salt, [PPN][{Au(ethisterone)$_2$}$_3$Cu$_2$] (**5**). While complex **5** was the major product of this reaction, small amounts of compound **4** were always present. Thus, the identity of **5** was confirmed by NMR spectroscopy and by comparison of its photophysical properties to those of analogous pentanuclear complexes with 1-ethynylcyclopentanol and 1-ethynylcyclohexanol ligands, [PPN][{Au(R)$_2$}$_3$Cu$_2$] **6** and **7** (**6**, R = 1-ethynylcyclopentanol; **7**, R = 1-ethynylcyclohexanol). These were prepared by the reaction of Au(I) complexes **2** and **3** with [Cu(MeCN)$_4$][PF$_6$] in a 3:1 ratio. Octanuclear Au_4Cu_4 complexes with the 1-ethynylcyclohexanol and 1-ethynylcyclopentanol ligands were unobtainable. Room temperature ^{1}H NMR spectra of **4**−**7** were complicated by the presence of aliphatic resonances, and therefore, ^{13}C NMR spectroscopy proved essential for characterization of the clusters. No resonances were observed for the alkyne carbons coordinated to Cu(I) ions in **4**, **6**, or **7**, but weak signals were seen in **5**. The pentanuclear complexes **5**−**7** (Chart 2) exhibited a single set of ligand resonances in the ^{13}C NMR spectrum, suggesting C_3 symmetry in solution. On the other hand, two distinct sets of ligand resonances were clearly visible for diagnostic protons (vinyl C*H*, O*H*, C*H*$_3$) in the ^{1}H NMR spectrum and for several resonances in the ^{13}C NMR spectrum of the Au_4Cu_4 complex **4** (see Supporting Information).

(51) Bagwoski, C. P.; You, Y.; Scheffler, H.; Vlecken, D. H.; Schmitza, D. J.; Ott, I. *Dalton Trans.* **2009**, 10799.
(52) Tiekink, E. R. T. *Crit. Rev. Oncol. Hematol.* **2002**, *42*, 225.
(53) McKeage, M. J.; Maharaj, L.; Berners-Price, S. J. *Coord. Chem. Rev.* **2002**, *232*, 127.
(54) Shaw, C. F. *Chem. Rev.* **1999**, *99*, 2589.
(55) Berners-Price, S. J.; Bowen, R. J.; Galettis, P.; Healy, P. C.; McKeage, M. J. *Coord. Chem. Rev.* **1999**, *185*−*6*, 823.
(56) Vicente, J.; Chicote, M. T.; Alvarez-Falcon, M. M.; Jones, P. G. *Organometallics* **2005**, *24*, 5956.
(57) Vicente, J.; Chicote, M. T.; Abrisqueta, M. D. *J. Chem. Soc., Dalton Trans.* **1995**, 497.
(58) McAdam, C. J.; Robinson, B. H.; Simpson, J. *Acta Crystallogr., Sect. C* **2007**, *63*, M338.

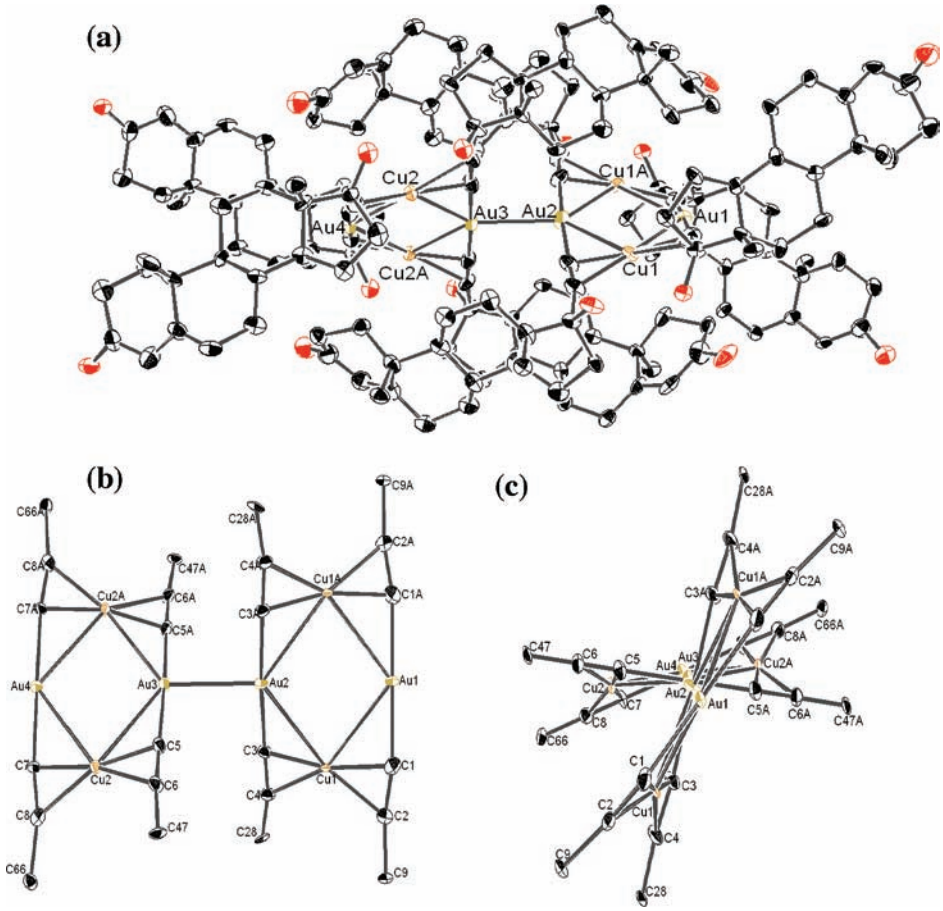

Figure 2. Perspective views of complex **4** displaying the (a) full structure, and the $[Au(acetylide)_2]_4$ Cu_4 core from (b) a side view, (c) end-on.

Chart 2

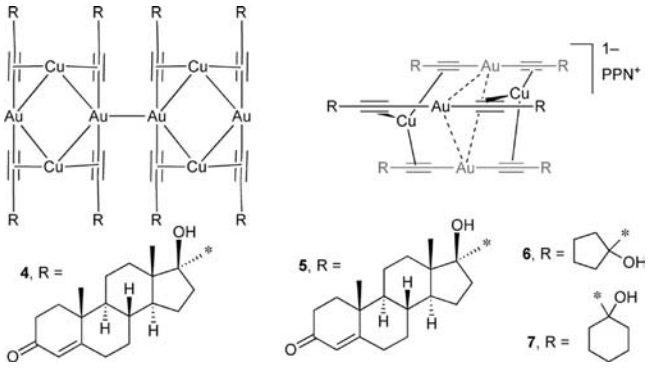

Complex **4**, $[\{Au(ethisterone)_2\}_4Cu_4]$, crystallizes in the chiral space group $P4_12_12$ as a dimer of $[\{Au(ethisterone)_2\}_2Cu_2]$ units connected by an unsupported Au···Au interaction having an exceptionally close contact of 2.927(1) Å which approaches the 2.889(1) Å Au···Au distance found in metallic gold. Within each Au_2Cu_2 unit, the Cu(I) ions bridge adjacent Au(I) bis(acetylide) anions by coordination to the acetylenic π bonds (Figure 2). The Cu−C distances in **4** range from 1.97(2) to 2.19(2) Å and Cu···Au separations range from 2.948(2) to 2.955(2) Å. Longer metal−metal separations of 3.919 and 3.870 Å are found between Au1···Au2 and Au3···Au4, indicative of the absence of any attractive interactions between these pairs of Au(I) ions. The linear orientation of the four Au(I) atoms and the relative positions of the acetylides are shown in Figure 2b. Dihedral angles between *adjacent* acetylides within each $[\{Au(ethisterone)_2\}_2Cu_2]$ unit (i.e., C1−Au1−Au2−C3) are approximately 26° while the C3−Au2−Au3−C5 dihedral angle between the Au···Au linked $[\{Au(ethisterone)_2\}_2Cu_2]$ units is nearly 81°. The packing of complex **4** contains large channels parallel to the *a*- and *b*-axes (see cif in Supporting Information). Recently, somewhat similar coordination has been reported for vapochromic $[Au_2Ag_2(4\text{-}C_6F_4I)_4]$ which can exist as a monomer or a polymer.[59] In the absence of acetylide donors, the Ag ions are coordinated only to the Au(I) ions.

Crystallization of clusters **6**, $[PPN][\{Au(ethynylcyclopentanol)_2\}_3Cu_2]$, and **7**, $[PPN][(Au\{ethynylcyclohexanol)_2\}_3Cu_2]$, from mixtures of CH_2Cl_2 and ether at −15 °C provided two different types of crystals of complex **6** and three different crystalline forms for complex **7**. Both forms of **6** were morphologically similar but were distinguishable by their blue (**6a**) or yellow-green (**6b**) solid-state emission (Figure 3). The three forms of cluster **7** were morphologically distinct with stacked blocks (blue emission, **7a**), needles (yellow-green emission, **7b**), and large blocks (yellow emission, **7c**). Form **7b** was the major product when the crystals were grown from CH_2Cl_2/ether in the freezer, while **7a** was present to the extent of ∼20% of the crystals, and **7c** existed as a small minority. Polymorph **7b** was obtained exclusively by slow evaporation of dichloromethane or by storing a solution of the complex in CH_2Cl_2 and hexanes (1:1 *v*:*v*) at −15 °C. Vapor diffusion of pentane into concentrated THF solutions yielded only crystals of **7c**. Recrystallization of isolated forms of **6** or **7** provided mixtures of each crystalline form. The complexes do not exhibit any luminescence mechanochromism or vapochromism.

(59) Laguna, A.; Lasanta, T.; Lopez-de-Luzuriaga, J. M.; Monge, M.; Naumov, P.; Olmos, M. E. *J. Am. Chem. Soc.* **2010**, *132*, 456.

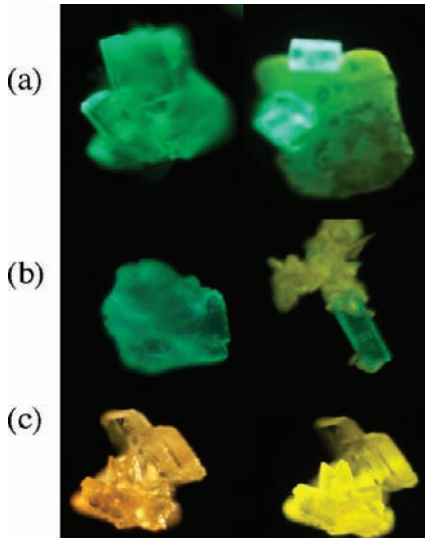

Figure 3. Photographs of crystals of (a) isolated **6a** (left), **6b** with two crystals of **6a** grown together (right), (b) **7a** on the left, and a mixture of **7b** (green) and **7c** (yellow) on the right, (c) isolated **7c** under ambient light (left) and UV irradiation (right). Slight differences in color between identical polymorphs are an artifact of brightness and focus.

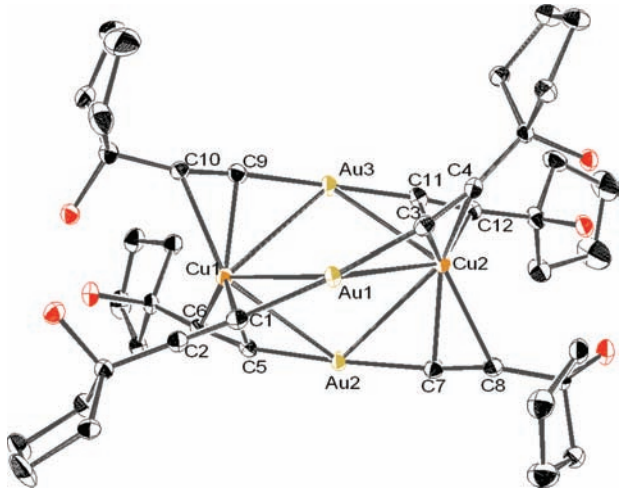

Figure 4. ORTEP diagram for **6a** with 40% thermal ellipsoids. Hydrogen atoms have been omitted.

The structures of **6a**, **6b**, **7a**, **7b**, and **7c** were determined crystallographically and each was found to adopt a geometry similar to those of aryl acetylide analogues reported in the literature.[19,21] Three Au(I) ions form a nearly equilateral triangle that is capped on both faces by Cu(I) ions to give a trigonal bipyramid of metal ions (Figure 4). Intramolecular Au···Au distances range from 3.2913(3) to 3.5917(3) Å, while Cu···Au distances span a minimum of 2.7876(7) Å to a maximum of 3.0502(7) Å with the smaller distances being somewhat shorter than the sum of van der Waals radii (3.06 Å) for Cu and Au. The extended structure exhibits intermolecular hydrogen bonding among −OH groups of the acetylide ligands. These complexes should be considered pseudopolymorphs as a variety of cocrystallized solvent molecules were found. Complex **6a** is solvent-free, but **6b** cocrystallized with four molecules of CH_2Cl_2, one of which is disordered with a PPN phenyl ring. For complex **7a** and **7b** each contains disordered CH_2Cl_2 and diethyl ether molecules, and **7c** contains two solvents per asymmetric unit. Detailed discussion regarding the treatment of disordered solvent molecules is described in the Experimental Section.

Significant differences between the polymorphic forms of **6** and **7** that appear to have spectroscopic consequences are found upon close examination of the Au···Au, Au···Cu, and Cu−C(acetylide) distances (Table 1). In **6a** the Au1···Au2 distance is 3.2913(1) Å, while the Au1···Au3 and Au2···Au3 distances are significantly longer (∼3.55−3.59 Å). Conversely, in **6b** a narrow distribution of Au···Au distances was found (3.4145(3)−3.4822(4) Å). For **7a** there are two Au···Au distances near 3.43 Å and one near 3.55 Å, while **7b** and **7c** exhibit one short and two long or two short and one long metal−metal distances, respectively. Smaller deviations among Au···Cu distances are found. The average Au···Cu distance in **6a** is slightly greater than that of **6b**, while **7c** exhibits the shortest and **7b** exhibits the longest average Au···Cu distances among the polymorphs of **7**. There are no significant differences in the sets of Au−C and alkynyl C−C distances between polymorphs of the same complex. In each complex, the distances between copper atoms and gold-bound carbon atoms (C_α) are somewhat shorter than the Cu−C_β distances, reflecting asymmetric coordination of the Cu(I) ions to the acetylide π system. This asymmetric coordination might be related to attractive forces between Cu and Au ions.

The structural results represent a rare example of luminescence polymorphism in which the same compound exhibits different color emissions based solely on differences in *intramolecular* bond lengths. The only *intermolecular* interactions are hydrogen bonds between −OH groups of the acetylide ligands, but the influence of intermolecular hydrogen bonding on intramolecular metal−metal distances can not be quantified easily. Importantly, the aliphatic portions of the acetylide ligands are not expected to be involved in the excited state. There is no interaction with the PPN cation or cocrystallized solvent in any of the pseudopolymorphs suggested here. Thus, different bond

Table 1. Selected Bond Lengths (Å) in Structures of **6** and **7**

	6a	6b	7a	7b	7c
Au1−Au2	3.2913 (3)	3.4273 (3)	3.4206 (5)	3.3728 (3)	3.3541 (3)
Au1−Au3	3.5462 (3)	3.4145 (3)	3.5496 (5)	3.5177 (3)	3.3330 (3)
Au2−Au3	3.5917 (3)	3.4822 (4)	3.4383 (5)	3.5123 (3)	3.5683 (3)
Cu1−Au1	2.8873 (5)	3.0495 (7)	3.0127 (8)	3.0502 (7)	2.7873 (6)
Cu1−Au2	2.9951 (5)	2.9140 (7)	2.9118 (7)	2.9280 (6)	3.0058 (6)
Cu1−Au3	3.0080 (5)	2.9635 (7)	2.9511 (7)	2.8969 (6)	2.9894 (6)
Cu2−Au1	2.9981 (5)	3.0205 (7)	3.0127 (8)	2.9459 (6)	2.9017 (6)
Cu2−Au2	2.9694 (5)	2.9545 (7)	2.9119 (7)	2.9528 (6)	3.0157 (7)
Cu2−Au3	2.9312 (5)	2.8137 (7)	2.9511 (7)	3.0493 (6)	2.8508 (7)
average Cu···Au	2.9648	2.9526	2.9585	2.9705	2.9251
average Cu−C_α	2.142	2.129	2.147	2.135	2.130
average Cu−C_β	2.333	2.414	2.359	2.403	2.443

Table 2. Summary of Photoluminescence Data

complex	absorptions/nm (ε/M^{-1} cm^{-1})	medium (T/K)	emission λ_{em}/nm (τ/μs)	Φ
4	230 (29,790), 305 (5,410)	CH_2Cl_2 (298)	496 (1.5)	0.65
	390 (5,703)	solid (298)	490 (1.1)	
		solid (77)	495 (1.9)	
5	250, 274, 297, 320[a]	CH_2Cl_2	570 (3.0)	0.06[b]
		solid (298)	499 (14)	
		solid (77)	516 (27)	
6	235 (45,580), 269 (16,540)	CH_2Cl_2 (298)	580 (8.9)	0.05
	276 (14,440), 295 (12,440)	**6a** solid (298)	504 (7.0)	
	320 (9,810)	**6a** solid (77)	515 (11)	
		6b solid (298)	530 (29)	
		6b solid (77)	540 (84)	
7	235 (76,420), 269 (21,890)	CH_2Cl_2 (298)	580 (21)	0.19
	276 (20,320), 295 (16,840)	**7a** solid (298)	505 (14)	
	320 (12,210)	**7a** solid (77)	526 (36)	
		7b solid (298)	548 (39)	
		7b solid (77)	562 (58)	
		7c solid (298)	555 (14)	
		7c solid (77)	578 (57)	

[a] Extinction coefficients are unknown as **5** was never completely void of small amounts of **4** and **1** (see below). [b] Approximate value.

lengths in the pseudopolymorphs of **6** and **7**, particularly Au···Au distances, are presumed responsible for the markedly different emissions from identical molecules.

In a reported example, [Au{cyclohexyl isocyanide}$_2$][PF_6] forms two different types of linear chains which are true polymorphs and differ by their Au···Au distances and emission color.[60,61] More typically, luminescence polymorphism arises from varying packing arrangements which may be accompanied by differing degrees of *inter*molecular interactions (i.e., metal−metal interactions or π stacking) which perturb the excited state.[62−70] In some cases, Au(I) cationic complexes which differ only by the anion or incorporation of different solvate molecules exhibit different emission properties related to the solid-state packing.[71,72] Balch and co-workers have shown that hexagold(I) complexes exhibit a phase change to a different polymorph that results in appreciable changes in aurophilic interactions and consequently drastically different emission at 298 K vs 77 K.[73]

Absorption and Emission Spectroscopy. Absorption and emission spectra of the Au_4Cu_4 cluster **4** are presented in Figure 5 and summarized in Table 2. The absorption spectrum is characterized by an intense band at 230 nm and two strong bands at 305 and 390 nm. The electronic spectra of the Au_3Cu_2 pentanuclear clusters **5**−**7** are characterized by strong absorptions at 230 nm and less intense shoulders ranging from 270 to 320 nm that decrease in intensity up to 350 nm (see Supporting Information). Spacings between the shoulders from 275 to 320 nm are on the order of 2300−2800 cm^{-1}, which may indicate vibronic structure in the optical transitions. Notably, the low-energy transitions in **5**−**7** are higher in energy than those reported for similar Au_3Cu_2 clusters.[21] High energy absorptions in other Au(I) acetylide complexes have been assigned as $^1(\pi-\pi^*)$ transitions of the acetylide ligand.[6,21,74,75] In consideration of the vibronic structure in the absorptions of **5**−**7**, a $^1(\pi-\pi^*)$ acetylide transition is plausible for these complexes as well. The weak absorptions at ∼350 nm extending toward the visible region may arise from cluster-centered (CC) or ligand-to-metal charge transfer (LMCT) contributions as their extinction coefficients drop substantially compared to the absorptions bands at $\lambda < 320$ nm and no particular maxima are apparent.

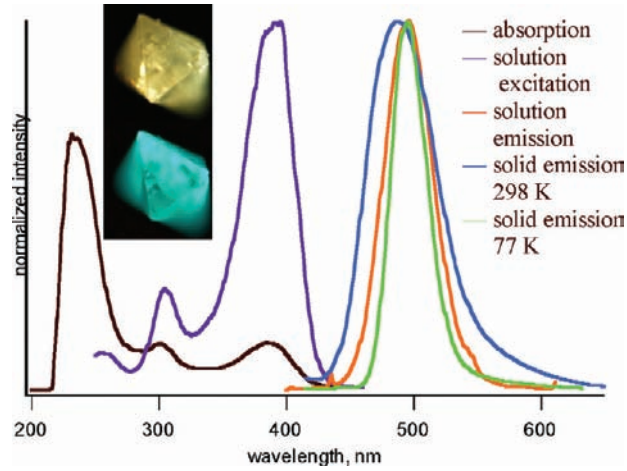

Figure 5. Absorption, excitation, and normalized emission spectra for complex **4**, [Au(ethisterone)$_2$]$_4$$Cu_4$, in CH_2Cl_2 (1×10^{-5} M) and in the solid state. Inset: Photographs of crystalline **4** under ambient light and UV irradiation at room temperature.

(60) White-Morris, R. L.; Olmstead, M. M.; Balch, A. L. *J. Am. Chem. Soc.* **2003**, *125*, 1033.
(61) Balch, A. L. *Gold Bull.* **2004**, *37*, 45.
(62) Zhang, G.; Lu, J.; Sabat, M.; Fraser, C. L. *J. Am. Chem. Soc.* **2010**, *132*, 2160.
(63) Zhang, H.; Zhang, Z.; Ye, K.; Zhang, J.; Wang, Y. *Adv. Mater.* **2006**, *18*, 2369.
(64) Mizukami, S.; Houjou, H.; Sugaya, K.; Koyama, E.; Tokuhisa, H.; Sasaki, T.; Kanesato, M. *Chem. Mater.* **2005**, *17*, 50.
(65) Gussenhoven, E. M.; Olmstead, M. M.; Fettinger, J. C.; Balch, A. L. *Inorg. Chem.* **2008**, *47*, 4570.
(66) White-Morris, R. L.; Olmstead, M. M.; Attar, S.; Balch, A. L. *Inorg. Chem.* **2005**, *44*, 5021.
(67) Toronto, D. V.; Weissbart, B.; Tinti, D. S.; Balch, A. L. *Inorg. Chem.* **1996**, *35*, 2484.
(68) Weissbart, B.; Toronto, D. V.; Balch, A. L.; Tinti, D. S. *Inorg. Chem.* **1996**, *35*, 2490.
(69) Kohmoto, S.; Tsuyuki, R.; Masu, H.; Azumaya, I.; Kishikawa, K. *Tetrahedron Lett.* **2008**, *49*, 39.
(70) Lu, W.; Zhu, N. Y.; Che, C. M. *J. Am. Chem. Soc.* **2003**, *125*, 16081.
(71) Rios, D.; Olmstead, M. M.; Balch, A. L. *Inorg. Chem.* **2009**, *48*, 5279.
(72) Rios, D.; Olmstead, M. M.; Balch, A. L. *Dalton. Trans.* **2008**, 4157.
(73) Gussenhoven, E. M.; Fettinger, J. C.; Pham, D. M.; Malwitz, M. M.; Balch, A. L. *J. Am. Chem. Soc.* **2005**, *127*, 10838.
(74) Yam, V. W. W.; Choi, S. W. K.; Cheung, K. K. *Organometallics* **1996**, *15*, 1734.
(75) Lu, W.; Xiang, H. F.; Zhu, N. Y.; Che, C. M. *Organometallics* **2002**, *21*, 2343.

Table 3. Calculated Energies, Oscillator Strengths (*f*), and Participating Orbitals for Complexes **4-C$_5$**,**4-Me,** and the Polymorphs of **6**, and **7**

complex	states	$\lambda_{calculated}$	energy (cm^{-1})	*f*	major orbitals
4-C$_5$	T_1	402.4	24849	0	HOMO→LUMO (100%)
	S_1	361.0	27702	0.5599	HOMO→LUMO (87%)
	S_2	338.3	29556	0.1016	HOMO−1→LUMO (85%)
4-Me	T_1	391.1	25184	0	HOMO→LUMO (102%)
	S_1	350.9	28501	0.6903	HOMO→LUMO (84%)
	S_2	332.1	30115	0.0041	HOMO−2→LUMO (33%)
					HOMO−1→LUMO (59%)
6a	T_1	391.8	25521	0	HOMO→LUMO (98%)
	S_1	373.8	26750	0.0013	HOMO→LUMO (96%)
6b	T_1	390.9	25580	0	HOMO→LUMO (96%)
	S_1	370.4	26995	0.0014	HOMO→LUMO (93%)
7a	T_1	393.1	25436	0	HOMO→LUMO (98%)
	S_1	372.9	26816	0.0002	HOMO→LUMO (96%)
7b	T_1	408.9	24453	0	HOMO→LUMO (96%)
	S_1	387.0	25841	0.0008	HOMO→LUMO (96%)
7c	T_1	379.0	26383	0	HOMO→LUMO (78%),
					HOMO−1→LUMO (19%)
	S_1	359.8	27796	0.0015	HOMO→LUMO (83%)
					HOMO−1→LUMO (13%)

Upon excitation into either absorption band of complex **4** in fluid CH_2Cl_2, emission at 496 nm ($\Phi = 0.65$, $\tau = 1.5$ μs) is observed. While the lifetime of 1.5 μs is suggestive of a triplet excited state, the emission of **4** is not quenched by oxygen. In dichloromethane, the pentanuclear clusters emit at 570 nm (**5**) and 580 nm (**6** and **7**) with quantum yields in the range of (0.05−0.19) and lifetimes of several microseconds (see Supporting Information for emission spectra). The similarity of solution emission energies for complexes **6** and **7** suggests that the saturated cyclopentyl and cyclohexyl rings are not involved in the excited state. Unlike complex **4**, the emission intensities of **5**−**7** are strongly attenuated in the presence of O_2.

All complexes exhibit bright solid-state emission at room temperature and at 77 K. For complex **4** a slight red shift from 490 to 495 nm is observed upon cooling from 298 to 77 K, while larger red shifts of 10−20 nm occur for the pentanuclear clusters **5**-**7**. Lifetimes at 77 K are somewhat longer than at room temperature. As shown in Figure 6, emission maxima for polymorphs **6a** and **6b** at 298 K differ by 26 nm (973 cm^{-1}), and polymorphs **7a** and **7b** exhibit emission maxima differing by 43 nm (1554 cm^{-1}). The energy difference is more subtle between **7b** and **7c** (7 nm, 230 cm^{-1}).

Electronic Structure Calculations. Time-dependent density functional (TD-DFT) calculations at the B3LYP/6-31G(d) level were performed on a simplified octanuclear complex [{Au(1-ethynylcyclopentanol)$_2$}$_4$Cu$_4$] (**4-C$_5$**) using the crystallographically determined geometry for complex **4**. This simplified model was used to reduce computational expense. The calculated parameters including the energy gap in wavenumbers and nm and the oscillator strength for the two lowest energy singlet states (S_1, S_2) and the lowest-energy triplet state (T_1) are listed in Table 3. All calculated transitions as well as the predicted absorption spectrum are provided as Supporting Information. From Figure 7 it can be seen that the highest occupied molecular orbital (HOMO) is composed mainly of Au and Cu d-orbitals with greater contributions from the Au2 and Au3 atoms that are connected by an unsupported aurophilic interaction along with some contribution from the acetylide π^b orbitals as well. The Au2···Au3 interaction in the HOMO is antibonding. The lowest unoccupied molecular orbital (LUMO), on the other hand, is composed principally of acetylide π^* functions and Au and Cu s and p orbitals. HOMO−1 consists of Au and Cu d-orbitals but is localized on only one of the two Au_2Cu_2 moieties. Inspection of HOMO−2 to HOMO−6 (Supporting Information) reveals nearly identical compositions for HOMO−1 and HOMO−2 with similar pairings of HOMO−3/−4 and HOMO−5/−6.

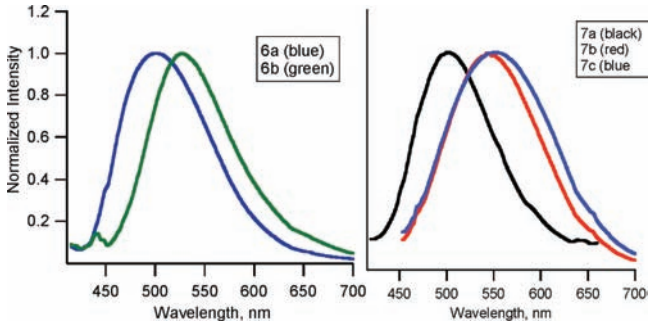

Figure 6. Solid-state emission spectra of the polymorphic forms of complexes **6** and **7** at room temperature.

We viewed the asymmetry in the HOMO−1/−2 pair of orbitals with some suspicion and were puzzled as to whether this might have been an artifact of the calculation. To probe this further, the structure was simplified to a methyl group set in place of the 1-cyclopentanol moiety to give [{Au(methyl acetylide)$_2$}$_4$Cu$_4$] (**4-Me).** While the orbital compositions and calculated transition energies remained similar to **4-C$_5$** (Figure 8), HOMO−1 and HOMO−2 are properly matched and are nearly degenerate (−6.19 and −6.20 eV). By matched, we mean that HOMO−1 is primarily located on the left half of the dimer, while HOMO−2 is nearly its mirror image. Likewise, HOMO−3/−4 and HOMO−5/−6 are paired spatially although energies are slightly different.

The calculated absorption spectrum of **4-Me** (Figure S24, Supporting Information) qualitatively matches the experimental absorption spectrum with the two lowest energy singlet absorptions attributed to the (1) HOMO→LUMO and (2) (HOMO−1 →LUMO) + (HOMO−2 →LUMO) transitions. Contributions from both HOMO−2 and HOMO−1 in the second excited state can be understood in terms of configuration mixing for these nearly degenerate orbitals. The similarity between experimental and calculated spectra supports the use of **4-Me** as a model for **4**, and implies orbitals of the steroid ligand are not involved in the lowest excited states. The orbital identities suggest an assignment of the excited state in **4** as cluster-centered ^{3}(CC)

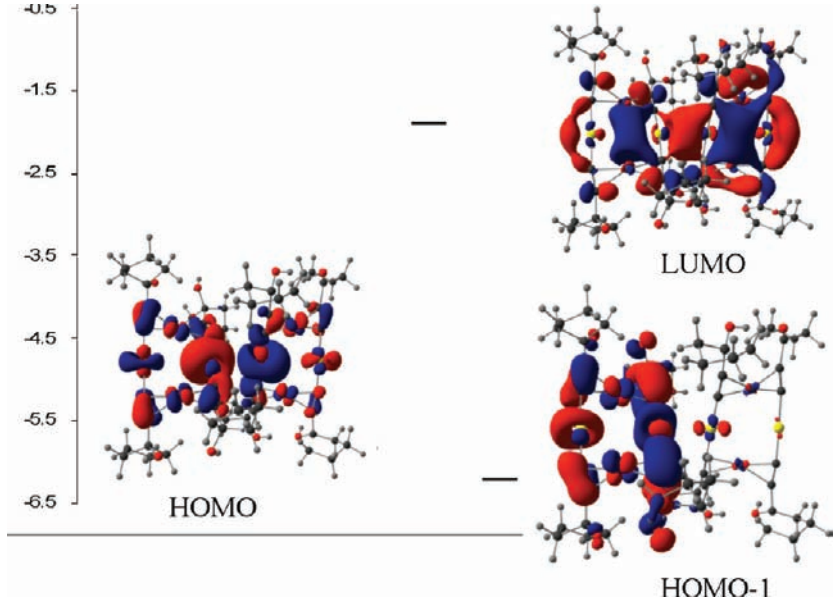

Figure 7. Calculated frontier orbitals and energies for complex **4-C$_5$**.

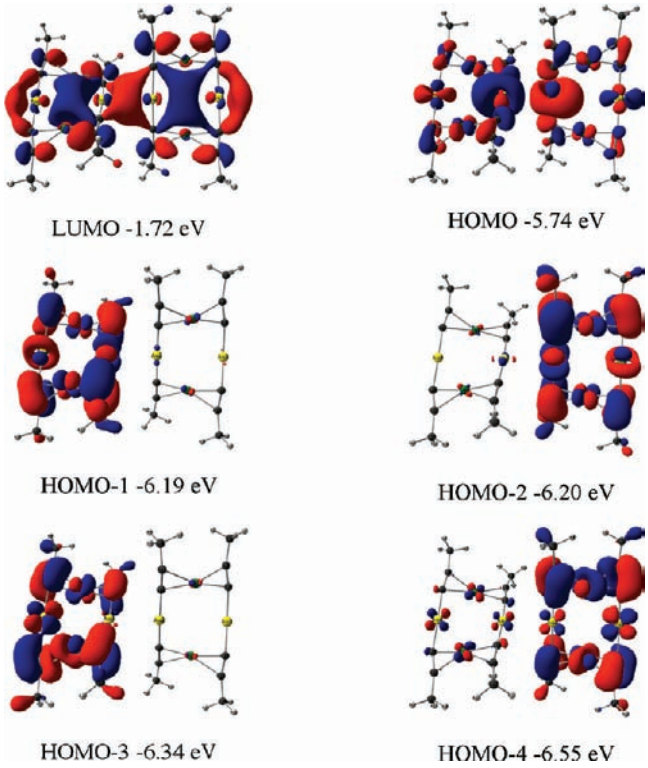

Figure 8. Frontier orbitals for complex **4-Me**. Isovalue = 0.025.

possibly mixed with some intraligand $^3(\pi-\pi^*)$ states. This assignment, in conjunction with a space-filling model of the complex (Figure S5, Supporting Information), offers a possible explanation for the absence of emission quenching by molecular oxygen in solution. Since the emissive core of the molecule is highly shielded by the eight steroid ligands, interaction of the luminophore with a quenching O_2 molecule is precluded.

A single point energy calculation of the lowest energy triplet state (T_1) was performed to model the electronic structure upon promotion of an electron from the highest occupied orbital to the LUMO. The ground state geometry was used for the calculation with the assumption that negligible geometry changes would occur in the solid state. As shown in Figure 9, the singly occupied orbitals (SOMOs) of T_1 are nearly identical in composition to the HOMO and LUMO of the singlet ground state, further supporting the excited-state assignment.

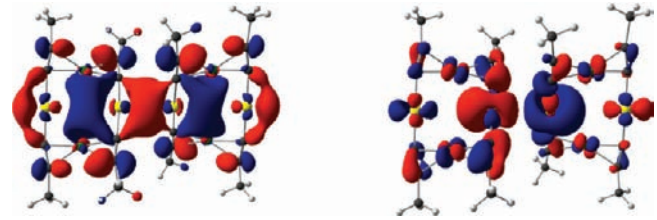

Figure 9. Frontier orbitals of the T_1 state of **4-Me** with the higher SOMO (−1.41 eV) on the left and the lower SOMO (−3.77 eV) on the right.

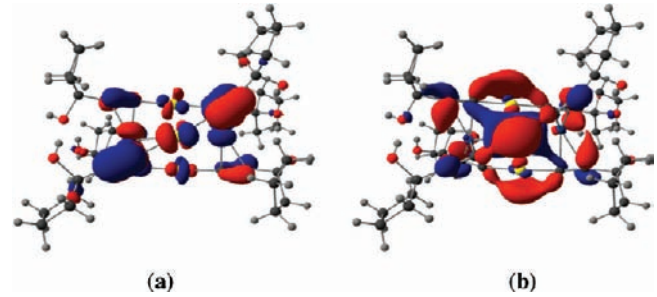

Figure 10. Calculated (a) HOMO (−2.7 eV) and (b) LUMO (1.41 eV) of polymorph **6a** [PPN][(Au(ethynylcyclopentanol)$_2$)]$_3$Cu$_2$.

Time-dependent DFT calculations for the pentanuclear clusters **6** and **7** indicate that the lowest-energy $S_0 \rightarrow S_1$ and $S_0 \rightarrow T_1$ transitions in these Au_3Cu_2 complexes are largely HOMO→LUMO in nature although slight mixing of HOMO−1→LUMO occurs to a modest extent in several of the compounds. Similar frontier orbitals were calculated for each polymorph of **6** and **7**. The HOMO is composed of gold and copper d orbitals and π^b-orbitals of the acetylide ligands, while the LUMO consists of gold sp-hybridized orbitals mixed with π^* orbitals of the acetylides (Figure 10). This description agrees with the reported electronic structure of [{Au(4-tolylacetylide)$_2$}$_3$M$_2$] (M = Cu, Ag) in which analysis of the frontier orbitals was used to explain the difference in emission energy

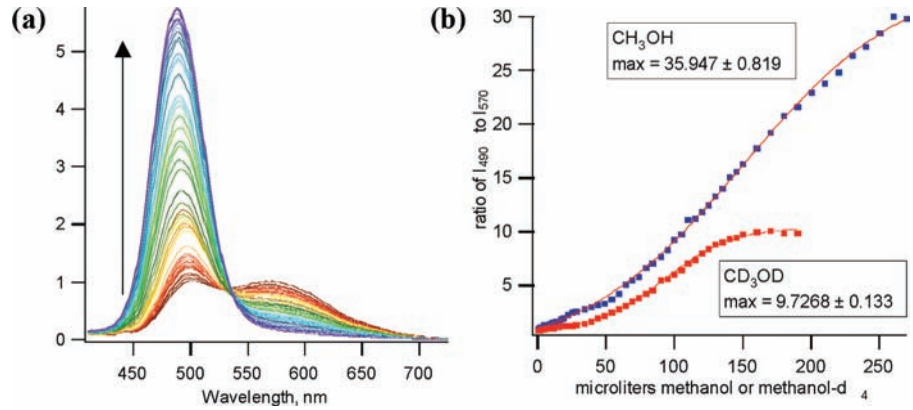

Figure 11. (a) Titration of **5** with methanol. Complex **5** emits at 570 nm, while complex **4** emits at 490 nm. λ_{exc} = 390 nm. (b) Ratio of the emission intensity at 490 to 570 during the titration of complex **5** with CH_3OH or CD_3OD.

between Ag(I) and Cu(I) congeners.[21] However, in the present work, analysis of the calculated HOMO/LUMO gaps does not clearly model the experimentally observed trends regarding solid-state emission energies between the polymorphs of **6** and **7** (**6a** > **6b** and **7a** > **7b** > **7c**). For complex **6**, only a difference of 161 cm^{-1} was calculated between the HOMO/LUMO gaps of the two polymorphs with a larger gap for **6b**. The HOMO/LUMO gap of **7c**, which exhibits yellow emission, is calculated to be 1,855 cm^{-1} *higher* in energy than that of the green emitting form, **7b**. Similar results were obtained using a simplified form of each complex $[PPN][Au_3Cu_2(C{\equiv}CCH_3)_6]$ with the core geometry of the parent compound. Analysis of the time-dependent calculations does not resolve the issue. As seen in Table 3, calculated T_1 and S_1 energies suggest very similar energy transitions for **6b** and **6a**. For complex **7** polymorphs, the calculations predict emission energies in the order: **7c** > **7a** > **7b**. The lowest-energy triplet states were calculated for the propyne models, $Au_3Cu_2(C{\equiv}CCH_3)_6$ to examine the singly occupied molecular orbitals. For complex **6a**, the triplet calculation did not converge; however in all other examples, the higher SOMO is identical to the ground state LUMO while the lower SOMO of T_1 is similar in composition to the ground state HOMO (Figures S33−S36, Supporting Information).

Although the HOMO/LUMO gaps or calculated absorption energies do not correlate with observed emission energies among polymorphs of clusters **6** and **7**, the DFT calculations provide insight in assigning the nature of the excited state as primarily ^{3}(CC) in **4** and as ligand-to-cluster charge transfer ^{3}(LCCT) in **5**−**7**. The contribution of the acetylides to the excited state is evident in the experimental absorption spectra of **5**−**7** which show some vibronic structure whereas the absorption in **4** exhibits broad bands.

In complexes **6** and **7**, Au···Au distances range from 3.2913(3) Å to 3.5917(3) Å with the latter generally believed to be outside the range of significant interactions. The variety in Au···Au distances is most likely responsible for the distinct differences in emission energy although subtle differences in Au···Cu distances may play a role. In light of the calculated nature of the HOMO and LUMO (i.e., metal−metal antibonding in the HOMO and metal−metal bonding character of the LUMO), closer Au···Au distances would be predicted to raise the HOMO and lower the LUMO although the extent of each effect is difficult to judge. This influence on the LUMO energy was found computationally with the exception of **7c.** The variety of Au···Au distances within each Au_3 triangle of a single complex compromises the ability to predict emission energy from crystallographic data.

While the luminescence polymorphism in these complexes arises from ligand-to-cluster charge transfer ^{3}(LCCT) states in triangular Au_3 cores, the assignment differs from that in other polymorphic Au(I) complexes in which linear AuR_2^+ cations are linked into chains by aurophilic interactions.[60] Complexes differing by the counteranion or cocrystallized solvent form extended structures in similar ways.[71,72] The aurophilic bonding in these types of aggregates arises from overlap of gold $5d_{z^2}$ orbitals to produce filled σ^b and σ^* MOs stabilized by configuration interaction with collinear empty p_z orbitals. The p_z orbitals form a similar but empty set of MOs. Excitation promotes an electron from the $5d_{z^2}$ σ^* band to the $6p_z$ σ^b band and therefore it would be anticipated that different Au···Au separations would affect the energy of this transition. In the present work on triangular Au^I_3 complexes, acetylide π-functions contribute strongly to the HOMO, while metal−metal antibonding contributions are small. Most similar to the Au(I) chains found in the literature is complex **4** with a linear arrangement of four Au(I) ions, two of which are quite close. In this case, the calculated highest occupied molecular orbital is indeed Au−Au *anti*-bonding with respect to the closely interacting Au(I) ions and the σ^b MO containing overlapping Au2−Au3 $5d_{z^2}$ orbitals, which was found to be MO number 114, (−9.37 eV, Figure S37, Supporting Information) is much lower in energy than the HOMO.

Equilibrium Between Complexes 4 and 5. During the preparation of crystallization solutions of $[PPN][\{Au(ethisterone)_2\}_3Cu_2]$ (**5**), it was noticed that the addition of some solvents (MeOH, EtOH, EtOAc, H_2O) to CH_2Cl_2 solutions of this pentanuclear complex resulted in a change in emission from yellow to the blue color characteristic of $[\{Au(ethisterone)_2\}_4Cu_4]$ (**4**). The yellow emission persisted in the presence of THF, pentane, hexanes, or ether. The process is reversible: if a few drops of MeOH are added, followed by dilution with CH_2Cl_2, the emission returns to yellow. Addition of more methanol results in blue emission again.

The ^{13}C NMR spectrum of **5** in CD_2Cl_2 displays major and minor components for some resonances in an approximate 10:1 ratio. Addition of CD_3OD (1:1 *v/v* with CD_2Cl_2) results in an increase of the minor component (Supporting Information). Upon standing overnight, the NMR solution provided crystals of **4**. Crystals of mononuclear **1** grew during slow evaporation of the remaining mother liquor.

A solution of **5** in dichloromethane was titrated with methanol and the emission spectra were recorded (Figure 11). With an increase in MeOH, the emission at 570 nm from complex **5**

decreases while the emission at 495 nm from complex **4** increases. A nearly isoemissive point occurs at 535 nm during the titration. The titration and ^{13}C NMR results may be explained by an equilibrium between complexes **5** and **4** + **1** (eq 1 where ethist = ethisterone). Formation of **4** thus appears to be favored in the presence of polar solvents capable of hydrogen-bonding either as H-bond donors or acceptors. To test this theory, methanol was added to yellow-emitting solution of **5** in CH_2Cl_2 to provide blue-emitting **4**. Complex **1** was then added to perturb the equilibrium and the yellow emission of **5** returned. The process was repeated by further addition of methanol then complex **1** to the same result. Addition of **1** to a pure solution of **4** resulted in formation of **5** as well.

$$2[PPN][\underset{\mathbf{5}}{\{Au(ethist)_2\}_3Cu_2}] \rightleftharpoons [\underset{\mathbf{4}}{\{Au(ethist)_2\}_4Cu_4}] + 2[PPN][\underset{\mathbf{1}}{Au(ethist)_2}] \quad (1)$$

The single set of impurity resonances in the ^{13}C NMR spectrum of **5** is likely an averaged signal resulting from rapid exchange between **4** and **1**. Otherwise, the impurity should be characterized by two resonances from pure **4** and one signal from free $Au(ethist)_2^-$.

Considering the nature of solvents that promote the formation of **4** and **1** from **5**, the response could result from a dielectric effect, a hydrogen-bonding driven process, or a combination of both. To probe the influence of hydrogen bonding, the titration of **5** in CH_2Cl_2 was performed with CH_3OH and CD_3OD in order to examine the extent to which complex **4** is formed from **5** in the presence of either solvent. The titration was carried out at 5×10^{-6} M, and the emission of the mixture was monitored using 390 nm as the excitation wavelength. To elucidate the effects of CH_3OH vs CD_3OD, the ratio of emission intensity at 490 nm (complex **4**) to the intensity at 570 nm (**5**) was plotted vs titrant volume.

The data from both titrations have been fit to sigmoidal curves (Figure 10b). For the MeOH titration, the maximum ratio of intensities at 490−570 nm is 35.9 ± 0.8 with half equivalence occurring at 150 μL of added methanol. When titrated with methanol-d_4, half equivalence is reached after 93 μL and the maximum ratio of intensities is calculated as 9.7 ± 0.1. Evidently, equilibrium (**1**) lies further to the right in the presence of protonated methanol relative to that in methanol-d_4. This observation is consistent with an equilibrium isotope effect in which H-bonding of **4** + **1** with solvent is more favorable for O−H than O−D *relative* to the zero-point energies of O−H and O−D in **5**.

Conclusions

Pentanuclear Au_3Cu_2 complexes with hydroxyl-aliphatic acetylide ligands can be prepared as PPN salts directly from Au(I) bis(acetylide) precursors and a Cu(I) source. When the acetylide is ethisterone, Au_3Cu_2 and Au_4Cu_4 clusters are obtained. The latter is a brightly emissive dimer exhibiting an unsupported aurophilic interaction between the central Au(I) atoms. $[PPN][\{Au(ethisterone)_2\}_3Cu_2]$ (**5**) is not particularly stable in solution and converts to the octanuclear complex (**4**) and the Au(I) bis(ethisterone) precursor (**1**) in a hydrogen-bonding assisted equilibrium which was probed by luminescence titration experiments. The octanuclear excited state is assigned as cluster-centered with particularly strong contribution from an anti-bonding Au2···Au3 interaction to the HOMO.

In the solid state, Au_3Cu_2 complexes with 1-cyclopentanol or 1-cyclohexanol alkynyl units exhibit an interesting example of luminescence polymorphism in which the color of emission varies, depending on the intramolecular atomic distances in the core of the clusters. The variety in distances may be influenced by a combination of attractive forces among closed-shell d^{10} Au(I) and Cu(I) ions and by intermolecular hydrogen-bonding schemes which were found to link the $Au_3Cu_2R_6$ complex anions into infinite chains in the solid state. Absorption and emission spectroscopy and lifetime measurements in conjunction with DFT calculations have led to an assignment of the excited state as ^{3}(acetylide π-to-Au_3Cu_2 cluster) charge transfer. With this assignment, different emission among polymorphs of the same complex can be understood as arising from some perturbation of the frontier orbitals evidenced by the different intramolecular $d^{10}-d^{10}$ M···M distances observed.

Experimental Section

General Considerations. NMR spectra were obtained using Bruker Avance 400 and 500 MHz spectrometers with ^1H and ^{13}C NMR chemical shifts referenced to residual solvent peaks in $CDCl_3$, CD_2Cl_2, or DMSO-d_6. $^{31}P\{^1H\}$ NMR data are referenced to external 85% H_3PO_4. Mass spectra of bis(acetylide) gold(I) ions were measured on a Shimadzu 2010 series liquid chromatography mass spectrometer (LC/MS) under negative mode electrospray ionization (ESI). Absorption spectra were measured on a Hitachi U-2000 UV−vis spectrometer. Steady-state excitation and emission spectra were obtained using a Spex Fluoromax-P fluorometer. Solution emission measurements were performed in quartz cuvettes equipped with screw-cap lids and septa, and samples were deoxygenated by purging with N_2 for at least 15 min prior to obtaining spectra. For titration experiments, deoxygenated methanol was added via 10 μL syringe to a deoxygenated CH_2Cl_2 solution of complex **4** through the septum. Solid-state emission samples were prepared by packing a capillary tube with the emissive complex in a matrix of KBr (~1% by wt). For low temperature measurements, the capillary was held in a vacuum dewar filled with liquid nitrogen. Lifetime measurements were performed using a model LN203C nitrogen laser (Laser Photonics Inc.) with λ = 337.1 nm and a 0.1 nm spectral width pulsed at 1 pulse/second. Signals were detected by a silicon photodiode and photomultiplier tube (1P28 type) with a 2 ns rise time and viewed with a Hewlett-Packard 54510-B oscilloscope connected to a computer *via* a GPIB interface. No less than five decay curves were averaged data fitting.

Syntheses were carried out under at atmosphere of N_2 using standard Schlenk conditions. Dichloromethane for reactions and photophysical measurements was dried by passage through an alumina solvent system. 1-ethynyl-1-cyclopentanol, 1-ethynyl-1-cyclohexanol, and ethisterone were purchased from Aldrich chemical company and used as received. $[PPN][Au(acac)_2]$ was prepared according to the literature.[76]

Crystal Structure Determinations. Each crystal was placed onto the tip of a glass fiber using Paratone and mounted on a Bruker SMART Platform diffractometer equipped with an APEX II CCD area detector. All data were collected at 100.0(1) K using Mo Kα radiation (graphite monochromator).[77] For each sample, a set of preliminary cell constants and an orientation matrix were determined from reflections harvested from three orthogonal wedges of reciprocal space. Full data collections were carried out with frame exposure times of 45 (**1**, **6a**, **6b**, **7b**, and **7c**), 60 (**2**, **3**, **7a**) or 90 (**4**) seconds at detector distances of 4 cm for **1**−**3**, **6a**, **6b**, and **7a**−**7c** or 6 cm for complex **4**. Randomly oriented regions of reciprocal space were surveyed for each sample: four major sections

(76) Vicente, J.; Chicote, M. T.; Saurallamas, I.; Lagunas, M. C. *J. Chem. Soc., Chem. Commun.* **1992**, 915.
(77) Saint Bruker AXS, Madison WI, 2008.

of frames were collected with 0.50° steps in ω at four different φ settings and a detector position of −38° in 2θ. The intensity data were corrected for absorption,[78] and final cell constants were calculated from the *xyz* centroids of approximately 4000 strong reflections from the actual data collection after integration.[77]

Structures were solved using SIR97[79] and refined using SHELXL-97.[80] Space groups were determined on the basis of systematic absences and intensity statistics. For complex **1**, a Paterson method solution was calculated which provided the location of the gold atoms from the E-map. For all other complexes, direct-methods solutions were calculated which provided most non-hydrogen atoms from the difference Fourier map. Full-matrix least-squares (on F^2)/difference Fourier cycles were performed which located the remaining non-hydrogen atoms which were refined with anisotropic displacement parameters. Absolute configurations for structures in chiral (**1**, **4**, **6b**) and noncentrosymmetric (**7b**) space groups were determined by anomalous dispersion effects. For complexes **1**, **2**, **6a**, and **7b**, hydroxide hydrogen atoms were found from the difference map and then refined as riding atoms with relative isotropic displacement parameters. For **6b**, **7a**, and **7c**, hydroxide hydrogen atoms could not be found and were placed in reasonable hydrogen-bonding positions on the basis of precedent in **6a** and **7b**. For **3**, all hydrogen atoms, and all nonhydroxide hydrogen atoms of all other structures were placed in ideal positions and refined as riding atoms with relative isotropic thermal parameters. For complex **4**, hydroxide hydrogen atoms were placed on the basis of residual peaks in the difference Fourier map prior to application of SQUEEZE;[81] one set is directed at the neighboring hydroxide oxygen atom, while the other is directed out into the solvent. Alkyne C−C bond lengths were restrained to be similar.

The cation and anion in **7a** are modeled as disordered over crystallographic mirror planes. One cocrystallized diethyl ether molecule is modeled as disordered over a mirror plane as well. Complex **7b** packs with a disordered combination of cocrystallized dichloromethane and diethyl ether molecules in channels parallel to the *c*-axis. One solvent site is modeled as a 45:55 disorder of one ether molecule and two dichloromethane molecules while the other site is modeled as 83:17 disorder of one diethyl ether molecule and one dichloromethane molecule. In **4** highly disordered cocrystallized solvent was found in channels parallel the *a*- and *b*-axes. In **7c** highly disordered solvent was found in four sites, each occupied by two solvent molecules. Reflection contributions from this solvent in **4** and **7c** were removed using the function SQUEEZE in the program PLATON which determined there to be 2097 electrons in 3975 Å^3 removed per unit cell in **4** and 355 electrons in 3975 Å^3 removed per unit cell in **7c**. Minor merohedral inversion twinning in **4** was refined to a mass ratio of 94:06.

Theoretical Calculations. DFT and time-dependent density functional (TD-DFT) calculations were carried out using the B3LYP[82,83] method as implemented by Gaussian 03.[84] The LANL2DZ[85−88] effective core potential was used for Au and Cu, while the 6-31G(d) basis set was applied for C, H, and O atoms. For the $[Au_3Cu_2]$ anionic polymorphs of complexes **6** and **7**, full geometries from the X-ray experiments were used. Additional single point calculations of the singlet (S_0) and triplet (T_1) states were performed on structures for which 1-cyclopentanol and 1-cyclohexanol moieties were replaced with methyl groups (**6a**-Methyl, **6b**-Methyl, etc.) Triplet calculations were performed using the restricted open shell method (roB3LYP) which forces $\alpha = \beta$. For the octanuclear complex, **4**, ethisterone ligands were reduced to 1-ethynylcyclopentanol (**4-C$_5$**) then further simplified to methyl acetylide (**4-Me**) in each case using the X-ray geometry for the core. TD-DFT was used to calculate the six lowest singlet and triplet energy absorptions from the S_0 state.

[PPN][Au(ethisterone)$_2$] (1). A mixture of [PPN][Au(acac)$_2$] (0.232 g, 0.25 mmol) and ethisterone (0.194 g, 0.62 mmol) was stirred in CH_2Cl_2 (15 mL) for 3 h covered with foil. The solution was filtered through Celite, concentrated to 1−2 mL, and added dropwise to 100 mL of rapidly stirring ether. The white precipitate was collected and dried to yield 0.310 g of **1** in 92% yield. X-ray-quality crystals were obtained by diffusion of diethyl ether into a CH_2Cl_2 solution of the complex. ^{1}H NMR (DMSO-d_6, 25 °C): δ 7.70−7.68 (m, 6H, PPN), 7.58−7.54 (m, 24H, PPN), 5.60 (s, 2H, =C*H*−), 4.39 (s, 2H, −O*H*), 2.39−2.34 (m, 4H, −C*H*−, −CH_2−), 2.22−2.11 (m, 4H −C*H*−, −CH_2−), 1.95−1.07 (m, 26H, −C*H*−, −CH_2−), 1.12 (s, 6H, −CH_3), 0.92−0.76 (m, 4H, −C*H*−, −CH_2−), 0.68 (s, 6H, CH_3). ^{13}C{^{1}H} NMR (CD_2Cl_2, 25 °C): δ 199.5 (s, quat), 172.4 (s, quat), 134.3 (s, Ar−*C*H), 132.7 (m, Ar−*C*H), 130.0 (m, Ar−*C*H), 127.6 (d, J = 108), 127.6 (s, ≡*C*−), 124.0 (s, −*C*H−, vinyl), 105.1 (s, ≡*C*−), 80.7 (s, quat), 53.7 (s, −*C*H−), 50.0 (s, −*C*H−), 46.8 (s, quat), 40.2 (s, −*C*H_2−), 39.2 (s, quat), 37.0 (s, −*C*H−), 36.1 (s, −*C*H_2−), 34.5 (s, −*C*H_2−), 33.5 (s, −*C*H_2−), 33.2 (s, −*C*H_2), 32.0 (s, −*C*H_2−), 23.6 (s, −*C*H_2−), 21.5 (s, −*C*H_2), 17.9 (s, −*C*H_3), 13.2 (s, −*C*H_3). ^{31}P{^{1}H} NMR (DMSO-d_6, 25 °C): δ 21.9 (s, PPN) MS (ESI negative) 819.15. Anal. Calc for $C_{78}H_{84}AuNO_4P_2 \cdot CH_2Cl_2$: C, 67.30; H, 6.12; N, 1.00. Found: C, 67.61; H, 6.23.

[PPN][[Au(1-ethynyl-cyclopentanol)$_2$] (2). To a CH_2Cl_2 (10 mL) solution of [PPN][Au(acac)$_2$] (0.163 g, 0.175 mmol) was added a CH_2Cl_2 (5 mL) solution of 1-ethynylcyclopentanol (0.059 g, 0.54 mmol). The reaction was covered with aluminum foil and stirred for 5 h. A white precipitate was collected and washed with CH_2Cl_2 (3 mL) and diethyl ether (50 mL) to provide 0.140 g of the title compound in 84% yield. Analytically pure, X-ray-quality crystals were grown by diffusion of diethyl ether into a dilute dichloromethane solution of the complex. ^{1}H NMR (DMSO-d_6, 25 °C): δ 7.71−7.69 (m, 6H, PPN), 7.60−7.53 (m, 24H, PPN), 4.42 (s, 2H, −O*H*), 1.63−1.53 (m, 16H, −CH_2−). ^{13}C{^{1}H} NMR (DMSO-d_6, 25 °C): δ 133.7 (s, PPN), 132.0 (m, PPN), 129.5 (m, PPN), 126.8 (d, J = 106, PPN), 125.1 (s, ≡C−), 106.0 (s, ≡*C*−), 73.1 (s, quat), 42.8 (s, −CH_2−), 23.1 (s, −CH_2−). ^{31}P{^{1}H} NMR (DMSO-d_6, 25 °C): δ 21.9 (s, PPN). MS (ESI negative) 414.95. *Anal.* Calc for $C_{50}H_{48}AuNO_2P_2$: C, 62.96; H, 5.07; N, 1.47. Found: C, 62.67; H, 4.91; N, 1.53.

[PPN][Au(1-ethynyl-cyclohexanol)$_2$] (3). A mixture of [PPN][Au(acac)$_2$] (0.244 g, 0.262 mmol) and 1-ethynylcyclohexanol (0.097 g, 0.79 mmol) was stirred in CH_2Cl_2 (10 mL) for 4 h covered with foil The solution was filtered through Celite, concentrated to 1−2 mL, and added to 75 mL of rapidly stirred ether to provide a fine white precipitate which was triturated for 1 h and collected by vacuum filtration to provide 0.200 g of product in 80% yield. X-ray-quality crystals were obtained by diffusion of diethyl ether into a CH_2Cl_2 solution of the complex. ^{1}H NMR (DMSO-d_6, 25 °C): δ 7.70−7.68 (m, 6H, PPN), 7.60−7.53 (m, 24H, PPN) 4.48 (s, 2H, −O*H*), 2.51−1.37 (m, 12H, −CH_2−), 1.36−1.28 (m, 6H, −CH_2−), 1.11−1.08 (m, 2H, −CH_2−). ^{13}C{^{1}H} NMR (DMSO-d_6, 25 °C): δ 133.6 (s, PPN), 131.9 (m, PPN), 129.5 (m, PPN), 126.8 (d, J = 107, PPN), 125.9 (s, ≡C−), 105.7 (s, ≡C−), 66.9 (s, quat), 41.1 (s, −*C*H_2−), 25.3 (s, −*C*H_2−), 23.0 (s, −*C*H_2−). ^{31}P{^{1}H} NMR (DMSO-d_6, 25 °C): δ 21.9 (s, PPN). MS (ESI negative) 443.00. *Anal.* Calc for $C_{52}H_{52}AuNO_2P_2$: C, 63.61; H, 5.34. Found: C, 63.05; H, 5.33.

[{Au(ethisterone)$_2$}$_4$Cu$_4$] (4). A mixture of **1** (0.100 g, 0.074 mmol) and $[Cu(MeCN)_4][PF_6]$ (0.024 g, 0.074 mmol) was stirred

(78) APEX2 Bruker AXS: Madison, WI, 2009.
(79) Altomare, A. B., M.C.; Camalli, M.; Cascarano, G. L.; Giacovazzo, C.; Guagliardi, A.; Moliterni, A. G. G.; Polidori, G.; Spagna, R. *Istituto di Cristallografio*, CNR: Bari, Italy, 1999.
(80) Sheldrick, G. M. *Acta Crystallogr.* **2008**, *A64*, 112.
(81) Spek, A. L.; *PLATON: A Multipurpose Crystallographic Tool*, version 300106; Utrecht University: Utrecht, The Netherlands, 2006.
(82) Becke, A. D. *J. Chem. Phys.* **1993**, *98*, 5652.
(83) Lee, C. T.; Yang, W. T.; Parr, R. G. *Phys. Rev. B* **1988**, *37*, 785.
(84) Frisch, M. J. T.; et al.; *Gaussian 03*, revision C.02; Gaussian, Inc.: Wallingford CT, 2004.
(85) Dunning, T. H. , Jr.; Hay, P. J. In *Modern Theoretical Chemistry*; Schaefer, H. F., III., Ed.; Plenum: New York, 1976; Vol. 3, pp 1−28.
(86) Hay, P. J.; Wadt, W. R. *J. Chem. Phys.* **1985**, *82*, 270.
(87) Hadt, W. R.; Hay, P. J. *J. Chem. Phys.* **1985**, *82*, 284.
(88) Hay, P. J.; Wadt, W. R. *J. Chem. Phys.* **1985**, *82*, 299.

for 3 h in 5 mL of CH_2Cl_2. The entire solution was set up for crystallization by vapor diffusion of ether into the CH_2Cl_2. After several days at room temperature, white flaky crystals were collected (0.055 g, 85%); however, NMR analysis revealed contamination by [PPN][PF_6]. Pure samples were obtained by vapor diffusion of ether into a solution of the complex in 1:1 *v*/*v* MeOH/CH_2Cl_2. ^{1}H NMR and microanalyses revealed the presence of ∼4 water molecules per complex *in the crystals*. This agrees with the presence of unknown solvent in the X-ray structure. ^{1}H NMR (CD_2Cl_2, 25 °C, 400 MHz): δ 5.94 (s, 4H, ═C*H*−), 5.69 (s, 4H, ═C*H*−), 4.49 (s, 4H, −O*H*), 3.82 (s, 4H, −O*H*), 2.65−1.25 (m, 136 H, −C*H*−, −CH_2−), 1.10−0.85 (m, 16H, −C*H*−, −CH_2−), 1.20 (s, 12H, −CH_3), 1.13 (s, 12H, −CH_3), 0.89 (s, 12H, −CH_3), 0.86 (s, 12H, −CH_3). ^{13}C{^{1}H} NMR (CD_2Cl_2, 25 °C, 400 MHz): δ 202.8 (s, quat), 199.6 (s, quat), 172.2 (s, quat), 171.2 (s, quat), 125.4 (s, −*C*H−, vinyl), 124.1 (s, −*C*H−, vinyl), 81.5 (s, quat), 80.9 (s, quat), ∼53.7 (s, −*C*H−, (overlapped with CD_2Cl_2), 50.5 (s, −*C*H−), 49.1 (s, −*C*H−), 48.2 (s, quat), 46.6 (s, quat) 42.2, 41.8, 39.5, 39.0, 36.9, 36.5, 36.2, 34.5, 34.3, 33.1, 32.3 (s, −*C*H_2−), 23.9 (s, −*C*H_2−), 23.6 (s, −*C*H_2−), 21.3 (s, −*C*H_2), 21.1 (s, −*C*H_2−), 17.7 (s, −*C*H_3), 13.3 (s, −*C*H_3). ^{31}P{^{1}H} NMR (CD_2Cl_2, 25 °C): δ 22.3 (s, PPN). *Anal.* Calc for $C_{168}H_{216}Au_4Cu_4O_{16}\cdot 4H_2O$: C, 55.96; H, 6.26. Found: C, 55.90; H, 6.32.

[PPN][{Au(ethisterone)$_2$}$_3$Cu$_2$] (5). A mixture of **1** (0.185 g, 0.14 mmol) and [Cu(MeCN)$_4$][PF_6] (0.030 g, 0.092 mmol) was stirred for 4 h in 5 mL of CH_2Cl_2. The volume was reduced to 2 mL, and diethyl ether was added to precipitate complex **5** and [PPN][PF_6] for a total of 0.194 g (97% for **5** · 2 [PPN]PF_6) ^{1}H NMR (CD_2Cl_2, 25 °C): δ 7.68−7.65 (m, 6H, PPN), 7.51−7.47 (m, 24H, PPN), 5.61 (s, 6H, ═C*H*−), 4.47 (s, 6H, −O*H*), 2.60−2.25 (m, 30 H, −C*H*−, −CH_2−), 2.00−1.26, (m, 60 H, −C*H*−, −CH_2−), 1.19−1.02 (m, 12H, −C*H*−, −CH_2−), 1.15 (s, 18H, −CH_3), 0.82 (s, 18H, −CH_3). ^{13}C{^{1}H} NMR (CD_2Cl_2, 25 °C): δ 199.4 (s, quat), 172.1 (s, quat), 134.3 (s, Ar−*C*H), 132.7 (m, Ar−*C*H), 130.0 (m, Ar-*C*H), 127.6 (d, J = 107), 124.0 (s, −*C*H−, vinyl), 115.3 (s, ≡C−), 111.8 (s, ≡C−), 81.3 (s, quat), 53.7 (s, −*C*H−), 50.1 (s, −*C*H−), 47.6 (s, quat), 39.2 (s, −*C*H_2−), 39.0 (s, quat), 37.1 (s, −*C*H−), 36.1 (s, −*C*H_2−), 34.5 (s, −*C*H_2−), 33.5 (s, −*C*H_2−), 33.0 (s, −*C*H_2), 32.0 (s, −*C*H_2−), 23.6 (s, −*C*H_2−), 21.4 (s, −*C*H_2), 17.8 (s, −*C*H_3), 13.5 (s, −*C*H_3). ^{31}P{^{1}H} NMR (CD_2Cl_2, 25 °C): δ 22.3 (s, PPN).

[PPN][{Au(1-ethynyl-cyclopentanol)$_2$}$_3$Cu$_2$] (6). Complex **2** (0.115 g, 0.121 mmol) and [Cu(MeCN)$_4$][PF_6] (0.026 g, 0.080 mmol) were stirred for 4 h in 6 mL of CH_2Cl_2. Ten milliliters of ether was added, and the mixture was filtered through a fine glass frit. The filtrate was left stored in the freezer whereupon crystals of **6a** (32 mg) and **6b** (32 mg) formed and were separated carefully by hand for a total of 64 mg (84% yield). ^{1}H NMR (DMSO-d_6, 25 °C): δ 7.71−7.60 (m, 6H, PPN), 7.60−7.52 (m, 24H, PPN), 5.20 (s, 6H, −O*H*), 1.84−1.80 (m, 24H, −CH_2−), 1.66−1.59 (m, 24H, −CH_2−) ^{13}C{^{1}H} NMR (CD_2Cl_2, 25 °C): δ 133.8 (s, PPN), 132.2 (m, PPN), 129.5 (m, PPN), 127.0 (d, J = 107, PPN), 75.9 (s, quat), 43.4 (s, −*C*H_2−), 23.5 (s, −*C*H_2−). ^{31}P{^{1}H} NMR (CD_2Cl_2, 25 °C): δ 22.4 (s, PPN). *Anal.* Calc for $C_{78}H_{84}Au_3Cu_2NO_6P_2$: C, 49.01; H, 4.43. Found: C, 48.84; H, 4.43.

[PPN][{Au(1-ethynyl-cyclohexanol)$_2$}$_3$Cu$_2$] (7). Complex **3** (0.045 g, 0.046 mmol) and [Cu(MeCN)$_4$][PF_6] (0.0099 g, 0.031 mmol) were stirred for 4 h in 5 mL of CH_2Cl_2, diluted with 10 mL of ether and filtered through a glass frit. The filtrate was stored in the freezer to provide a mixture of **7a**, **7b**, and **7c** which were collected by centrifugation and washed with diethyl ether to yield 0.026 g (85% yield) of complex **7** as a mixture of polymorphs. Individual polymorphs were obtained as described in the synthesis section. ^{1}H NMR (CD_2Cl_2, 25 °C): δ 7.67−7.58 (m, 6H, PPN), 7.51−7.43 (m, 24H, PPN), 1.98−1.90 (m, 12H, −CH_2−), 1.57−1.16 (m, 42H, −CH_2−), 1.16−1.13 (m, 6H, −CH_2−). ^{1}H NMR (DMSO-d_6, 25 °C): δ 7.70−7.57 (m, 6H, PPN), 7.57−7.54 (m, 24H, PPN), 5.41 (br, 6H, −O*H*), 1.78 (m, 10H, −CH_2−), 1.52−1.15 (m, 42H, −CH_2−), 1.14−1.07 (m, 8H, −CH_2−). ^{13}C{^{1}H} NMR (CD_2Cl_2, 25 °C): δ 133.7 (s, PPN), 132.1 (m, PPN), 129.5 (m, PPN), 127.0 (d, J = 108, PPN), 69.4 (s, quat), 40.4 (s, −*C*H_2−), 25.5 (s, −*C*H_2−), 23.5 (s, −*C*H_2−). ^{31}P{^{1}H} NMR (CD_2Cl_2, 25 °C): δ 22.4 (s, PPN). *Anal.* Calc for $C_{84}H_{96}Au_3Cu_2NO_6P_2$: C, 50.56; H, 4.85. Found: C, 50.35; H, 5.04.

Acknowledgment. Professor Tom Cundari (U. of North Texas) and Dr. Theresa McCormick are gratefully acknowledged for fruitful discussions concerning DFT calculations. We thank Christopher M. Evans for assistance with lifetime measurements and crystal photographs, and the National Science Foundation GOALI program (Grant CHE-0616782) for support of this research.

Supporting Information Available: Complete reference 84, ORTEP diagrams, refinement parameters, and packing diagrams for **1**, **2**, **4**, **6a**, **6b**, **7a**, **7b**, **7c**, space filling diagram for **4**, crystallographic data in cif format, absorption, excitation, emission for **4**, **5**, **6**, **7**, calculated absorption spectra and transition lists for **4-C$_5$** and **4-Me**, triplet orbitals for **4-Me**, frontier orbital diagrams and tables of all calculated transitions for **6a**, **6b**, **7a**, **7b**, **7c**, orbital diagrams for S_0 and T_1 of simplified **6a**, **6b**, **7a**, **7b**, **7c**, ^{1}H and ^{13}C NMR of complexes with ethisterone (**1**, **4**, **5**) This material is available free of charge via the Internet at http://pubs.acs.org.

JA103400E